THE JOURNAL OF PHYSICAL CHEMISTRY LETTERS
A JOURNAL OF THE AMERICAN CHEMICAL SOCIETY

pubs.acs.org/JPCL Letter

Synthesis and Electrochemical Properties of Aluminum Hexafluorophosphate

Xiaoyu Wen, Jian Zhang, Hewei Luo,* Jiayan Shi, Charlene Tsay, Huanhuan Jiang, Ying-Hsuan Lin, Marshall A. Schroeder, Kang Xu, and Juchen Guo*

Cite This: *J. Phys. Chem. Lett.* 2021, 12, 5903−5908 Read Online

ACCESS | Metrics & More | Article Recommendations | Supporting Information

ABSTRACT: We report the first synthesis of aluminum hexafluorophosphate ($Al(PF_6)_3$) and its electrochemical properties in dimethyl sulfoxide (DMSO). The single crystal structure of the synthesized $Al(PF_6)_3$ is revealed as $[Al(DMSO)_6](PF_6)_3$, and 0.25 M $Al(PF_6)_3$ in DMSO with high ionic conductivity is obtained. The purity of this electrolyte was further confirmed with nuclear magnetic resonance spectroscopy and electrospray ionization mass spectrometry. We then demonstrated the reversibility of Al deposition−stripping in this electrolyte using scanning electron microscopy and an X-ray photoelectron spectroscopy depth profiling study. The parasitic reaction involving DMSO decomposition during Al deposition is also identified via gas chromatography/electron ionization mass spectrometry.

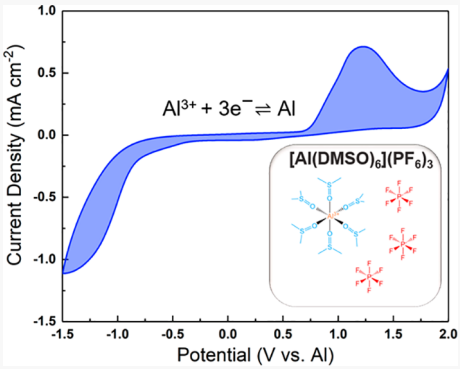

While battery chemistries using multivalent cations as working ions have always been tantalizing due to the potential multiplication of capacity and energy density they promise, the high valence of these ions also introduce tremendous challenges in terms of solvation, transport, and kinetics across interfaces. The multivalent cations investigated thus far were mostly confined to bivalent ions such as Zn^{2+}, Mg^{2+}, or Ca^{2+},[1,2] while the trivalent ions such as aluminum (Al^{3+}) still remain beyond the horizon.

To date, the electrochemical deposition of Al can only be achieved in electrolytes based on highly corrosive aluminum halides, mainly aluminum chloride ($AlCl_3$).[3−6] Regardless of the formulas of the electrolytes, which are either $AlCl_3$-containing deep eutectic systems of molten salt or $AlCl_3$ solutions in organic solvents, the only active species known to deposit Al are Lewis acidic chloroaluminate anions $Al_2Cl_7^-$ and $Al_3Cl_{10}^-$, with the former being the predominantly reported species in the literature.[7−10] The corrosive nature of the chloride makes the chloroaluminate electrolytes impractical, particularly for the emerging research on rechargeable Al batteries.[11,12] A number of studies have also indicated that the chloroaluminate electrolytes are not chemically compatible with transition metal oxide, chloride, or sulfide cathode materials.[13−16] Furthermore, the anodic stability of the chloroaluminate electrolytes is limited by the oxidation of chloride, which occurs at fairly low potential and generates highly toxic and even more corrosive gaseous chlorine.[17] Therefore, the development of chloride-free Al electrolytes is critical to the development of rechargeable Al batteries.

Al electrolytes based on weakly coordinating anions could provide solutions that circumvent the disadvantages of chloroaluminate electrolytes. Mandai et al.[18] and Reed et al.[19] studied the commercially available aluminum trifluoromethanesulfonate ($Al(CF_3SO_3)_3$) in *N*-methylacetamide (with urea additive) and diglyme, respectively. Although the $Al(CF_3SO_3)_3$ electrolytes exhibited wider electrochemical window than the chloroaluminate electrolytes, they demonstrate little reactivity of Al deposition and stripping. It is believed that the ionic bonding between the $CF_3SO_3^-$ anion and Al^{3+} cation is still too strong to achieve effective dissociation. Al bis(trifluoromethanesulfonyl)imide ($Al(TFSI)_3$) was synthesized by Chiku et al. using $AlCl_3$ and bis(trifluoromethanesulfonyl]amine as the reactants in acetonitrile (MeCN).[20] The main Al-containing species in the obtained electrolyte was identified as $[Al(TFSI)_x(MeCN)_{6-x}]^{3-x}$ (non-fully dissociated $Al(TFSI)_3$ solvated by MeCN) from spectroscopic characterizations. Certain reversible electrochemical behavior was demonstrated, however, without unambiguous evidence of Al deposition and stripping. Among the common weakly coordinating anions, the hexafluorophosphate (PF_6^-) anion, which has predominantly been used in the Li-ion battery industry, emerges as the natural

Received: April 16, 2021
Accepted: June 17, 2021

https://doi.org/10.1021/acs.jpclett.1c01236
J. Phys. Chem. Lett. 2021, 12, 5903−5908

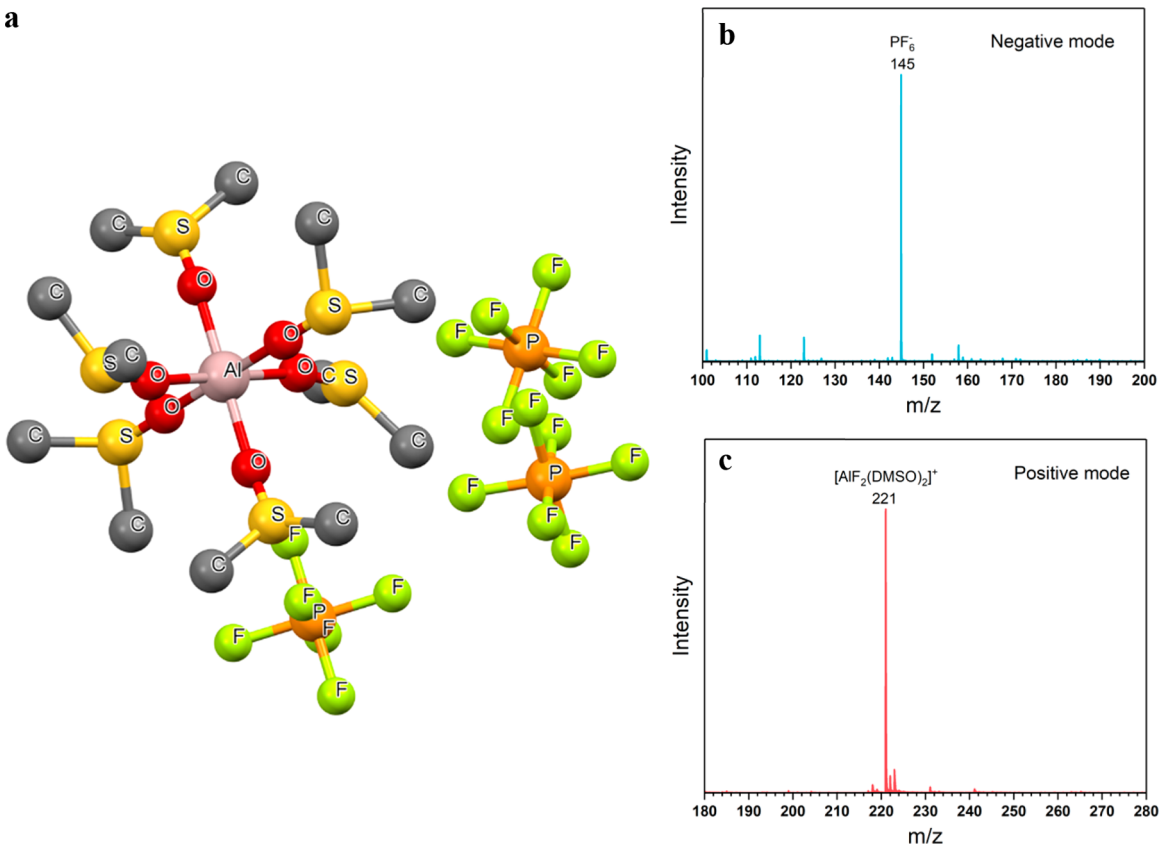

Figure 1. (a) Single crystal structure of $[Al(DMSO)_6](PF_6)_3$ (hydrogen atoms omitted for clarity). ESI-MS spectra of $[Al(DMSO)_6](PF_6)_3$: (b) negative mode and (c) positive mode.

choice as it strikes a good balance between dissociation constant and mobility as well as stability.[21] In this study, we report the successful synthesis of an $Al(PF_6)_3$ electrolyte for the first time and its preliminary yet encouraging electrochemical properties.

$Al(PF_6)_3$ was synthesized through the reaction between ammonium hexafluorophosphate (NH_4PF_6) and triethylaluminum (Et_3Al) as shown in reaction 1.

$$Et_3Al + 3NH_4PF_6 \rightarrow Al(PF_6)_3 + 3NH_3 \uparrow + 3C_2H_6\uparrow \quad (1)$$

The experimental details can be found in the Supporting Information. The selection of the solvent of this reaction was restricted by the compatibility with Et_3Al and solubility of $Al(PF_6)_3$: Et_3Al is very reactive toward olefinic groups, carbonyls, primary and secondary amines, hydroxyl groups, and so on.[22] One may also anticipate that the especially strong Coulombic attraction between the trivalent Al^{3+} and the PF_6^- anion renders it much more difficult for the ion solvation to sufficiently compensate for energy loss during the disruption of the rather stable $Al(PF_6)_3$ lattice. Eventually, we identify dimethyl sulfoxide (DMSO) as the only proper solvent that meets the above stringent requirements, with both good solvation power for $Al(PF_6)_3$ and chemical stability with Et_3Al.

After the synthesis, the single crystals of $Al(PF_6)_3$ were obtained from a saturated solution of $Al(PF_6)_3$ in DMSO (0.25 M) by slow evaporation of DMSO at 90 °C for 2 days. The structure of the single crystal as determined by X-ray diffraction analysis (Figure 1a) reveals that $Al(PF_6)_3$ consists of Al^{3+} cations coordinated by six DMSO molecules. Three PF_6^- anions are located at ∼6.6 Å from the Al^{3+} cation. The detailed crystal structure information about $[Al(DMSO)_6](PF_6)_3$ can be found in the Supporting Information. The ionic species in the electrolyte were characterized by using electrospray ionization mass spectrometry (ESI-MS). Figure 1b shows the negative mode of the spectrum, where the dominant peak at 144.9 m/z can clearly be attributed to the PF_6^- anion. In the positive mode spectrum the dominant peak at 221.0 m/z (Figure 1c) is attributed to the $[AlF_2(DMSO)_2]^+$ cationic fragment. We believe this was generated from the ionization of $[Al(DMSO)_6](PF_6)_3$ with uncharged phosphorus pentafluoride (PF_5) as the other product, which cannot be directly detected by mass spectrometer because of its electroneutrality. As such, the fragmentation during ionization is proposed as reaction 2.

$$[Al(DMSO)_6](PF_6)_3 \rightarrow [AlF_2(DMSO)_2]^- + 2PF_5 + PF_6^- + 4DMSO \quad (2)$$

Overall, the neatness of both positive and negative modes of ESI-MS, each with only one dominant peak, strongly confirms the high purity of $Al(PF_6)_3$ synthesized in this work. The content of Al and phosphorus (P) in the $Al(PF_6)_3$ salt was also analyzed with inductively coupled plasma optical emission spectroscopy (ICP-OES). The obtained P/Al molar ratio is 3.014, which is in excellent agreement with the theoretical ratio in $Al(PF_6)_3$.

The ionic conductivity of 0.25 M $Al(PF_6)_3$ electrolyte in DMSO was measured as ∼1.2×10^{-2} S cm^{-1} at room temperature, which, in comparison with the typical ion conductivity of lithium ion electrolytes (10^{-3}–10^{-2} S cm^{-1}), is sufficient to support ion transport in bulk electrolytes.

https://doi.org/10.1021/acs.jpclett.1c01236
J. Phys. Chem. Lett. 2021, 12, 5903−5908

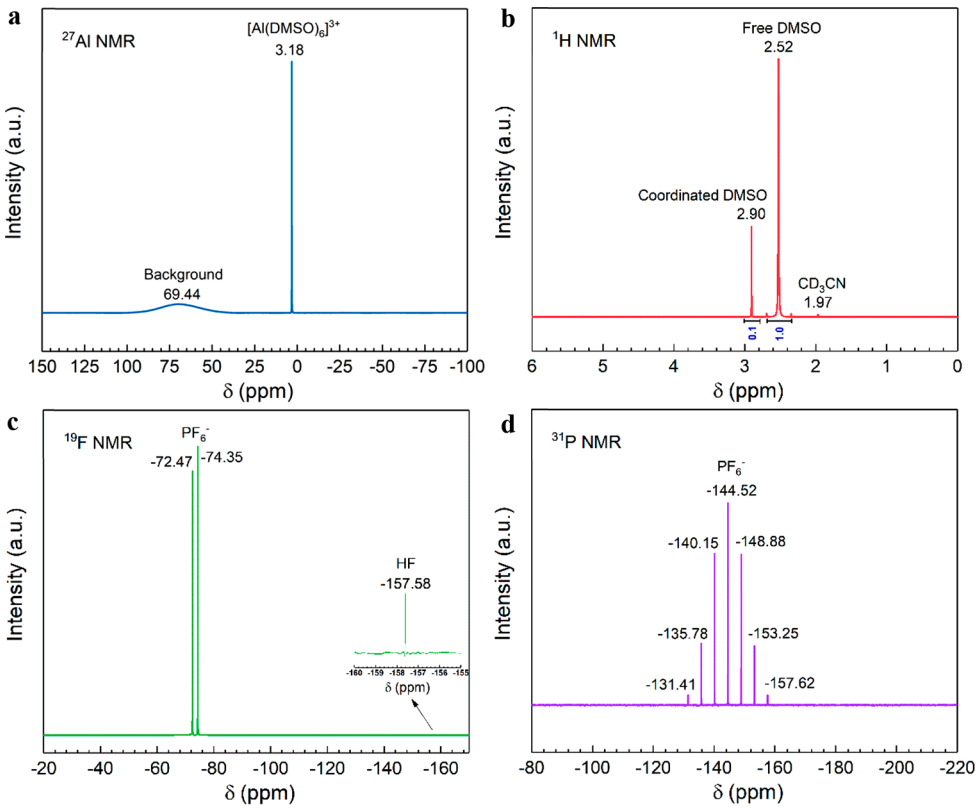

Figure 2. (a) ^{27}Al, (b) ^{1}H, (c) ^{19}F, and (d) ^{31}P NMR spectra of the 0.25 M $Al(PF_6)_3$ electrolyte in DMSO.

The composition of the electrolyte solution was further identified through liquid-state nuclear magnetic resonance (NMR) spectroscopy. The ^{27}Al NMR spectrum (Figure 2a) shows a sharp peak at 3.18 ppm corresponding to the Al^{3+} cations coordinated by six DMSO molecules (in a 6-coordination environment).[23] No Al peak associated with Et_3Al was detected. In Figure 2b, the ^{1}H NMR spectrum shows two close singlets assigned to free DMSO at 2.52 ppm[24] and DMSO coordinated to Al^{3+} at 2.90 ppm. The integration ratio of coordinated DMSO to free DMSO is 1:10, which matches very well with the calculation based on the concentration (0.25 M). The ^{19}F (Figure 2c) and ^{31}P NMR spectra (Figure 2d) demonstrate the existence of PF_6^- anions with high purity. The doublet signal of PF_6^- in ^{19}F NMR at −72.47 and −74.35 ppm occurred due to a ^{19}F−^{31}P coupling. Accordingly, the septet signal in the ^{31}P NMR spectrum from −131 to −158 ppm represents PF_6^-.[25] There were no major impurities detected in any of the NMR spectra; however, a very small peak in the ^{19}F NMR at −157.58 ppm was observed and attributed to hydrogen fluoride (HF).[26] The existence of HF in solutions of hexafluorophosphate salts (e.g., $LiPF_6$,[27,28] $NaPF_6$,[29] and $Mg(PF_6)_2$[30]) seems to be inevitable and is well documented due to the existence of trace amounts of water in the solution, despite the DMSO solvent used in this work has been thoroughly dried and purified before use.

The cyclic voltammogram (CV) of the $Al(PF_6)_3$ electrolyte obtained on a platinum working electrode in a three-electrode electrochemical cell is shown in Figure 3a (red curve). The CV scan of 0.1 M $LiPF_6$ in DMSO in the same potential window does not show any noticeable redox peaks (Figure S1 in the Supporting Information). Therefore, the cathodic peak at approximately −1.0 V and the anodic peak at 1.3 V (both versus Al) in the CV curve correspond to the reversible Al deposition−stripping. The chronopotentiometry curve of Al deposition on copper (Cu) working electrode at 0.15 mA cm^{-2} is plotted in Figure 3b (red curve), which demonstrates a stable overpotential of approximately −1.1 V versus Al until it rapidly increases after the 4 h mark. The deposition was characterized by using a scanning electron microscope (SEM) with energy dispersive X-ray (EDX) spectroscopy and X-ray photoelectron spectroscopy (XPS). As the SEM image in Figure 3c displays, the deposit obtained from the 0.25 M $Al(PF_6)_3$ in DMSO was small particles dispersed on the Cu substrate. The ^{27}Al, ^{1}H, ^{19}F, and ^{31}P NMR spectra of the electrolyte after deposition (Figure S2) show no major compositional changes; however, the ^{27}Al NMR spectrum reveals the appearance of hydrated Al^{3+} cations ($Al(H_2O)_6^{3+}$), and the ^{19}F NMR spectrum indicates an increase in the HF concentration. Both observations indicate that the trace amount of water in the electrolyte causes parasitic reactions during the electrochemical deposition. Aurbach et al. previously demonstrated that a small amount of reducing agent, such as di-*n*-butylmagnesium, could effectively remove trace amount of water and lead to highly reversible Mg deposition−stripping in the Mg-ion electrolyte.[31] With a similar strategy, we added 250 ppm Et_3Al to the 0.25 M $Al(PF_6)_3$ electrolyte. Indeed, in the presence of Et_3Al which serves as a water scavenger, the peak current of both peaks in the deposition−stripping CV (blue curve in Figure 3a) was significantly increased, and the overpotential of Al stripping was lowered by 0.7 V compared to the pristine electrolyte. The overpotential of the chronopotentiometry deposition of Al was also reduced by 0.5 V after the addition of Et_3Al, as presented in Figure 3b (blue curve). Furthermore, the distinctly different surface morphology of the Al deposit after the addition of Et_3Al is shown in Figure 3d. Unlike the particle deposit from

https://doi.org/10.1021/acs.jpclett.1c01236
J. Phys. Chem. Lett. 2021, 12, 5903−5908

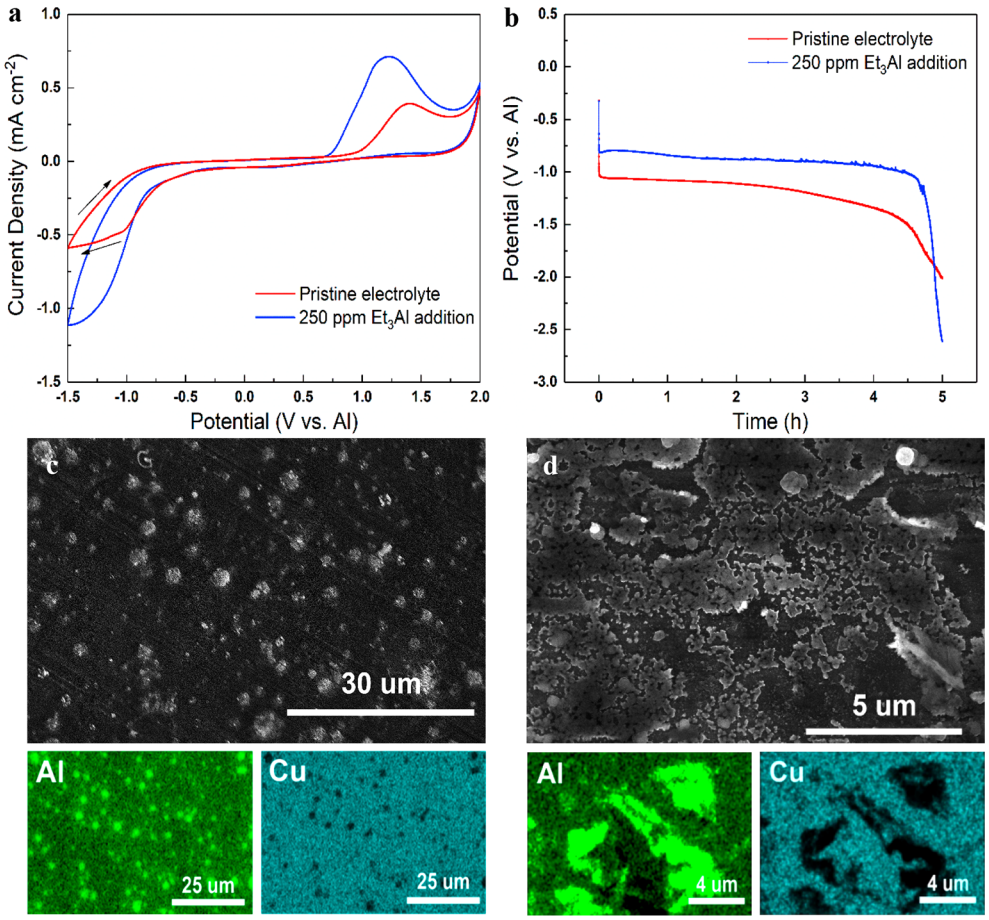

Figure 3. (a) CV scans at 25 mV s^{-1} in 0.25 M $Al(PF_6)_3$ in DMSO with and without 250 ppm Et_3Al additive. (b) Chronopotentiometry curve at −0.15 mA cm^{-2} with and without 250 ppm Et_3Al additive; SEM images and EDX elemental mapping of Al deposit on Cu from 0.25 M $Al(PF_6)_3$ in DMSO (c) without and (d) with 250 ppm Et_3Al additive.

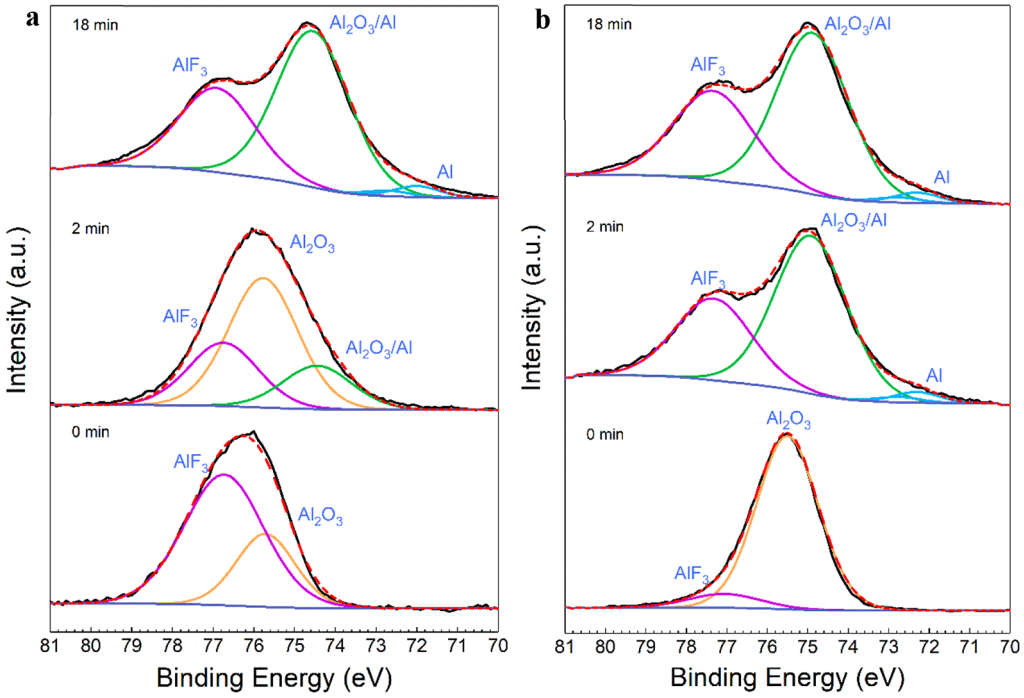

Figure 4. Al 2p XPS depth profiling analysis of the Al deposits from the electrolytes of 0.25 M $Al(PF_6)_3$ in DMSO (a) without and (b) with 250 ppm Et_3Al additive.

https://doi.org/10.1021/acs.jpclett.1c01236
J. Phys. Chem. Lett. 2021, 12, 5903−5908

the pristine electrolyte, the deposit from the Et_3Al-enhanced electrolyte formed layers over a large area, suggesting a more uniform and efficient electrodeposition process. The EDX elemental mappings clearly display the distribution of the Al element on the Cu substrate (full spectra are in Figure S3).

The Al deposition was further analyzed with XPS to identify the composition of the deposits. Figure 4a shows Al 2p XPS spectra with depth profiling after electrodeposition from electrolyte without the Et_3Al additive. Two deconvoluted peaks at 77.0 and 75.8 eV in the spectrum of the pristine surface (0 min argon sputtering) were attributed to aluminum fluoride (AlF_3) and aluminum oxide (Al_2O_3), respectively.[32] After sputtering for 2 min with argon ions, the relative intensity of the AlF_3 peak decreased compared to that of Al_2O_3. Additionally, a new peak at 74.8 eV, which can be assigned to the thin Al_2O_3 layer on metallic Al,[33] emerged in the spectrum. After sputtering for 18 min, the peak at 75.8 eV representing the thick Al_2O_3 layer diminished in the Al 2p spectrum. Meanwhile, the relative intensity of the thin Al_2O_3 layer on metallic Al peak significantly increased. Furthermore, a pair of peaks at 72.6 eV (Al $2p_{3/2}$) corresponding to metallic Al emerged in the spectrum.[34] These observations indicate that the deposition of metallic Al occurs simultaneously with the formation of Al_2O_3 during the initial period of deposition. The Al and Al_2O_3 may subsequently react with the HF impurity in the $Al(PF_6)_3$ electrolyte to form AlF_3, which appeared close to the surface of the deposit. Adding Et_3Al significantly alleviated the formation of AlF_3, as shown in Figure 4b. Compared to the pristine surface deposited from the electrolyte without Et_3Al, the surface layer from the electrolyte with Et_3Al shows a weaker AlF_3 signal. More importantly, the peaks of metallic Al emerged after only 2 min of sputtering in the absence of peaks representing the thick Al_2O_3 layer. These XPS results further confirm that the addition of Et_3Al facilitates Al deposition by removing H_2O and the related parasitic reactions due to HF. Unfortunately, the formation of Al_2O_3 seems an inherent parasitic reaction of Al deposition regardless of whether Et_3Al was added.

The possible mechanism of Al_2O_3 formation was probed by using gas chromatography/electron ionization mass spectrometry (GC/EI-MS) (spectrum shown in Figure S4) during the chronopotentiometry deposition of Al. In both electrolytes with and without Et_3Al, gaseous dimethyl sulfide (C_2H_6S) was detected with GC/EI-MS during Al deposition. Therefore, the side reaction (or one of the side reactions) involving the reduction of DMSO during electrodeposition is proposed as reaction 3.

$$2Al^{3+} + 6e^- + 3C_2H_6OS \rightarrow Al_2O_3 + 3C_2H_6S\uparrow \quad (3)$$

Our work demonstrates the first successful synthesis of the chloride-free Al electrolyte based on the weakly coordinating PF_6^- anion. Electrochemical deposition−stripping of Al from the electrolyte of $Al(PF_6)_3$ in DMSO was demonstrated to be reversible, particularly after removal of the water impurity by the addition of a small amount of Et_3Al. We also found that Al deposition−stripping is undermined by the continuous cathodic decomposition of DMSO on the electrode surface to form Al_2O_3. It remains a challenge to find better solvents for $Al(PF_6)_3$ that must be able to dissolve the salt while being chemically and electrochemically stable. The future strategies should focus on the substitution of PF_6^- with a more weakly coordinating and stable anion that can be dissolved in the solvent with better cathodic stability.

■ ASSOCIATED CONTENT

Supporting Information

The Supporting Information is available free of charge at https://pubs.acs.org/doi/10.1021/acs.jpclett.1c01236.

Experimental details, CV scan of 0.1 M $LiPF_6$ in DMSO, ^{27}Al, ^{1}H, ^{19}F, and ^{31}P NMR spectra of the electrolyte after Al deposition, EDX spectra of the Al deposition, GC/EI-MS spectrum of the gaseous product during Al deposition, crystal data and structure refinement of $[Al(DMSO)_6](PF_6)_3$ (PDF)

■ AUTHOR INFORMATION

Corresponding Authors

Hewei Luo − *School of Material and Chemical Engineering, Zhengzhou University of Light Industry, Zhengzhou 450002, China*; Email: luohw@zzuli.edu.cn

Juchen Guo − *Department of Chemical and Environmental Engineering and Materials Science and Engineering Program, University of California, Riverside, Riverside, California 92521, United States*; orcid.org/0000-0001-9829-1202; Email: juguo@ucr.edu

Authors

Xiaoyu Wen − *Department of Chemical and Environmental Engineering, University of California, Riverside, Riverside, California 92521, United States*

Jian Zhang − *Materials Science and Engineering Program, University of California, Riverside, Riverside, California 92521, United States*; orcid.org/0000-0003-0356-7611

Jiayan Shi − *Department of Chemical and Environmental Engineering, University of California, Riverside, Riverside, California 92521, United States*; orcid.org/0000-0001-8432-240X

Charlene Tsay − *Department of Chemistry, University of California, Riverside, Riverside, California 92521, United States*

Huanhuan Jiang − *Department of Chemical and Environmental Engineering and Department of Environmental Sciences, University of California, Riverside, Riverside, California 92521, United States*; orcid.org/0000-0002-5581-375X

Ying-Hsuan Lin − *Department of Environmental Sciences, University of California, Riverside, Riverside, California 92521, United States*; orcid.org/0000-0001-8904-1287

Marshall A. Schroeder − *Energy Sciences Division, US Army Research Laboratory, Adelphi, Maryland 20783, United States*; orcid.org/0000-0002-8160-2833

Kang Xu − *Energy Sciences Division, US Army Research Laboratory, Adelphi, Maryland 20783, United States*; orcid.org/0000-0002-6946-8635

Complete contact information is available at: https://pubs.acs.org/10.1021/acs.jpclett.1c01236

Notes

The authors declare no competing financial interest.

■ ACKNOWLEDGMENTS

X.W. and J.G. acknowledge the financial support from U.S. National Science Foundation (NSF) CAREER program through Grant CBET-1751929. NMR measurements were performed at the Analytical Chemistry Instrumentation Facility at UCR, funded in part by NSF under Grant CHE-1626673.

XPS was performed at the UC Irvine Materials Research Institute (IMRI) using instrumentation funded in part by the National Science Foundation Major Research Instrumentation Program under Grant CHE-1338173. M.A.S. and K.X. acknowledge the support from DOE Office of Science via Joint Center of Energy Research under IAA SN2020957 and Dr. Yue Li (University of Maryland) for assistance with the ESI-MS measurements. The authors also thank Mr. David Lyons (University of California - Riverside) for the ICP-OES measurements.

■ REFERENCES

(1) Ma, L.; Schroeder, M. A.; Borodin, O.; Pollard, T. P.; Ding, M. S.; Wang, C.; Xu, K. Realizing High Zinc Reversibility in Rechargeable Batteries. *Nature Energy* **2020**, *5*, 743−749.

(2) Sun, W.; Wang, F.; Zhang, B.; Zhang, M.; Kupers, V.; Ji, X.; Theile, C.; Bieker, P.; Xu, K.; Wang, C.; Winter, M. A Rechargeable Zinc-Air Battery Based on Zinc Peroxide Chemistry. *Science* **2021**, *371*, 46−51.

(3) Ferrara, C.; Dall'Asta, V.; Berbenni, V.; Quartarone, E.; Mustarelli, P. Physicochemical Characterization of $AlCl_3$−1-Ethyl-3-methylimidazolium Chloride Ionic Liquid Electrolytes for Aluminum Rechargeable Batteries. *J. Phys. Chem. C* **2017**, *121*, 26607−26614.

(4) Wang, H.; Gu, S.; Bai, Y.; Chen, S.; Zhu, N.; Wu, C.; Wu, F. Anion-Effects on Electrochemical Properties of Ionic Liquid Electrolytes for Rechargeable Aluminum Batteries. *J. Mater. Chem. A* **2015**, *3*, 22677−22686.

(5) Coleman, F.; Srinivasan, G.; Swadzba-Kwasny, M. Liquid Coordination Complexes Formed by the Heterolytic Cleavage of Metal Halides. *Angew. Chem., Int. Ed.* **2013**, *52*, 12582−6.

(6) Li, M.; Gao, B.; Liu, C.; Chen, W.; Shi, Z.; Hu, X.; Wang, Z. Electrodeposition of Aluminum from $AlCl_3$/Acetamide Eutectic Solvent. *Electrochim. Acta* **2015**, *180*, 811−814.

(7) Jiang, T.; Chollier Brym, M. J.; Dubé, G.; Lasia, A.; Brisard, G. M. Electrodeposition of Aluminium from Ionic Liquids: Part I—Electrodeposition and Surface Morphology of Aluminium from Aluminium Chloride ($AlCl_3$)−1-ethyl-3-methylimidazolium chloride ([EMIm]Cl) ionic liquids. *Surf. Coat. Technol.* **2006**, *201*, 1−9.

(8) Wang, Q.; Zhang, Q.; Lu, X.; Zhang, S. Electrodeposition of Al from Chloroaluminate Ionic Liquids with Different Cations. *Ionics* **2017**, *23*, 2449−2455.

(9) Pradhan, D.; Reddy, R. G. Mechanistic Study of Al Electrodeposition from EMIC−$AlCl_3$ and BMIC−$AlCl_3$ Electrolytes at Low Temperature. *Mater. Chem. Phys.* **2014**, *143*, 564−569.

(10) Wen, X.; Liu, Y.; Xu, D.; Zhao, Y.; Lake, R. K.; Guo, J. Room-Temperature Electrodeposition of Aluminum via Manipulating Coordination Structure in $AlCl_3$ Solutions. *J. Phys. Chem. Lett.* **2020**, *11*, 1589−1593.

(11) Tseng, C.-H.; Chang, J.-K.; Chen, J.-R.; Tsai, W. T.; Deng, M.-J.; Sun, I. W. Corrosion Behaviors of Materials in Aluminum Chloride−1-Ethyl-3-Methylimidazolium Chloride Ionic Liquid. *Electrochem. Commun.* **2010**, *12*, 1091−1094.

(12) Reed, L. D.; Menke, E. The Roles of V_2O_5 and Stainless Steel in Rechargeable Al−Ion Batteries. *J. Electrochem. Soc.* **2013**, *160*, A915−A917.

(13) Wen, X.; Liu, Y.; Jadhav, A.; Zhang, J.; Borchardt, D.; Shi, J.; Wong, B. M.; Sanyal, B.; Messinger, R. J.; Guo, J. Materials Compatibility in Rechargeable Aluminum Batteries: Chemical and Electrochemical Properties between Vanadium Pentoxide and Chloroaluminate Ionic Liquids. *Chem. Mater.* **2019**, *31*, 7238−7247.

(14) Donahue, F. M.; Mancini, S.; Simonsen, L. Secondary Aluminium-Iron (III) Chloride Batteries with a Low Temperature Molten Salt Electrolyte. *J. Appl. Electrochem.* **1992**, *22*, 230−234.

(15) Mori, T.; Orikasa, Y.; Nakanishi, K.; Kezheng, C.; Hattori, M.; Ohta, T.; Uchimoto, Y. Discharge/Charge Reaction Mechanisms of FeS_2 Cathode Material for Aluminum Rechargeable Batteries at 55° C. *J. Power Sources* **2016**, *313*, 9−14.

(16) Zafar, Z. A.; Imtiaz, S.; Razaq, R.; Ji, S.; Huang, T.; Zhang, Z.; Huang, Y.; Anderson, J. A. Cathode Materials for Rechargeable Aluminum Batteries: Current Status and Progress. *J. Mater. Chem. A* **2017**, *5*, 5646−5660.

(17) Shi, J.; Zhang, J.; Guo, J. Avoiding Pitfalls in Rechargeable Aluminum Batteries Research. *ACS Energy Letters* **2019**, *4*, 2124−2129.

(18) Mandai, T.; Johansson, P. AI Conductive Haloaluminate-Free Non-Aqueous Room-Temperature Electrolytes. *J. Mater. Chem. A* **2015**, *3*, 12230−12239.

(19) Reed, L. D.; Arteaga, A.; Menke, E. J. A Combined Experimental and Computational Study of an Aluminum Triflate/Diglyme Electrolyte. *J. Phys. Chem. B* **2015**, *119*, 12677−12681.

(20) Chiku, M.; Matsumura, S.; Takeda, H.; Higuchi, E.; Inoue, H. Aluminum Bis (trifluoromethanesulfonyl)imide as a Chloride-Free Electrolyte for Rechargeable Aluminum Batteries. *J. Electrochem. Soc.* **2017**, *164*, A1841.

(21) Xu, K. Nonaqueous Liquid Electrolytes for Lithium-Based Rechargeable Batteries. *Chem. Rev.* **2004**, *104*, 4303−4418.

(22) Marsel, C. J.; Kalil, E. O.; Reidlinger, A.; Kramer, L. Preparation and Ignition Properties of Aluminum Alkyls. In *Metal-Organic Compounds*; American Chemical Society: 1959; Vol. *23*, pp 172−183.

(23) Martineau, C.; Taulelle, F.; Haouas, M. The Use of ^{27}Al NMR to Study Aluminum Compounds: a Survey of the Last 25 Years. *PATAI'S Chemistry of Functional Groups* **2009**, 1−51.

(24) Gottlieb, H. E.; Kotlyar, V.; Nudelman, A. NMR Chemical Shifts of Common Laboratory Solvents as Trace Impurities. *J. Org. Chem.* **1997**, *62*, 7512−7515.

(25) Parimalam, B. S.; MacIntosh, A. D.; Kadam, R.; Lucht, B. L. Decomposition Reactions of Anode Solid Electrolyte Interphase (SEI) Components with $LiPF_6$. *J. Phys. Chem. C* **2017**, *121*, 22733−22738.

(26) Wilken, S.; Treskow, M.; Scheers, J.; Johansson, P.; Jacobsson, P. Initial Stages of Thermal Decomposition of $LiPF_6$-Based Lithium Ion Battery Electrolytes by Detailed Raman and NMR Spectroscopy. *RSC Adv.* **2013**, *3*, 16359−16364.

(27) Barlowz, C. Reaction of Water with Hexafluorophosphates and with Li Bis (perfluoroethylsulfonyl) imide Salt. *Electrochem. Solid-State Lett.* **1999**, *2*, 362−364.

(28) Lux, S. F.; Chevalier, J.; Lucas, I. T.; Kostecki, R. HF Formation in $LiPF_6$-Based Organic Carbonate Electrolytes. *ECS Electrochem. Lett.* **2013**, *2*, A121−A123.

(29) Dahbi, M.; Nakano, T.; Yabuuchi, N.; Fujimura, S.; Chihara, K.; Kubota, K.; Son, J. Y.; Cui, Y. T.; Oji, H.; Komaba, S. Effect of Hexafluorophosphate and Fluoroethylene Carbonate on Electrochemical Performance and the Surface Layer of Hard Carbon for Sodium-Ion Batteries. *ChemElectroChem* **2016**, *3*, 1856−1867.

(30) Keyzer, E. N.; Glass, H. F.; Liu, Z.; Bayley, P. M.; Dutton, S. E.; Grey, C. P.; Wright, D. S. $Mg(PF_6)_2$-Based Electrolyte Systems: Understanding Electrolyte-Electrode Interactions for the Development of Mg-Ion Batteries. *J. Am. Chem. Soc.* **2016**, *138*, 8682−8685.

(31) Shterenberg, I.; Salama, M.; Yoo, H. D.; Gofer, Y.; Park, J.-B.; Sun, Y.-K.; Aurbach, D. Evaluation of $(CF_3SO_2)_2N$−(TFSI) Based Electrolyte Solutions for Mg Batteries. *J. Electrochem. Soc.* **2015**, *162*, A7118−A7128.

(32) Hess, A.; Kemnitz, E.; Lippitz, A.; Unger, W.; Menz, D. ESCA, XRD, and IR Characterization of Aluminum Oxide, Hydroxyfluoride, and Fluoride Surfaces in Correlation with Their Catalytic Activity in Heterogeneous Halogen Exchange Reactions. *J. Catal.* **1994**, *148*, 270−280.

(33) Yan, Y.; Helfand, M.; Clayton, C. Evaluation of the Effect of Surface Roughness on Thin Film Thickness Measurements Using Variable Angle XPS. *Appl. Surf. Sci.* **1989**, *37*, 395−405.

(34) Sarapatka, T. Palladium-Induced Charge Transports with Palladium/Alumina/Aluminum Interface Formation. *J. Phys. Chem.* **1993**, *97*, 11274−11277.

https://doi.org/10.1021/acs.jpclett.1c01236
J. Phys. Chem. Lett. 2021, 12, 5903−5908